Available online at www.eccomasproceedia.org
Eccomas Proceedia SMART (2023) 1458-1469

ECCOMAS
Proceedia

X ECCOMAS Thematic Conference on Smart Structures and Materials
SMART 2023
D.A. Saravanos, A. Benjeddou, N. Chrysochoidis and T. Theodosiou (Eds)

PERFROMANCE ANALYSIS AND MODELING OF BIO-INSPIRED 3D-ARRAYS FOR THERMAL MANAGEMENT

NIKOLAOS ATHANASOPOULOS[1*], GRIGORIOS M. CHATZIATHANASIOU[1,2] AND NIKOLAOS SIAKAVELLAS[2]

[1*]Institute of Chemical Engineering Scienses (ICE/HT),
Foundation of Research and Technology (FORTH)
Stadiou Str, Platani Rion, Patras
GR- 26504, Greece
*e-mail: n.athanasopoulos@iceht.forth.gr, nikos_athanasopoulos@protonmail.com

[2]University of Patras, Department of Mechanical Engineering & Aeronautics,
Patras, 26500, Greece

Abstract. The thermo-optical properties of common materials cannot change significantly as a function of temperature. However, holistic and mechanistic strategies have been adopted by Nature in order to control the temperature of a body. Photonastic and thermonastic movements are realized in order to transform the shape of leaves and petals under light or temperature stimulus. The different thermo-optical properties of the leaves' external skin, as well as the folding of leaves control the sunlight absorption in order to prevent overheating and damages. We have developed smart surfaces which manipulate passively and very efficiently the thermal emission of a body. The smart surfaces consist of smaller unit-cells. The transformation of the geometry of the unit cells, reveals or conceals different thermo-optical properties and changes the view factor of the smart surface in order to alter its effective emissivity. The arrays transform their shape via their anisotropic structure and the developed thermal stresses, which occur because of the large thermal expansion (CTE) mismatch of the highly oriented polyethylene and the other layers of the material. We investigated numerically the effective emissivity as a function of the temperature dependent CTE and modulus (E) of the material. The temperature dependent properties enhance the performance at lower temperature levels. However, the heat rejection capability remains high at temperatures below 90 ^{o}C. Also, we investigated thoroughly how the thermal conductivity of the outer layer affects the shape of the smart surface's unit-cells and the thermal rejection performance. Finally, we calculated the directional emissivity at different temperature levels.

Key words: Bio-inspired materials, Thermal management, Smart surfaces, FE modelling, Thermal radiation, Space applications

Peer-review under responsibility of the organizing committee of SMART 2023.
doi: 10.7712/150123.9917.455503

1 INTRODUCTION

Advanced electrochromic materials [1,2], active micro-electromechanical systems [3] and active metamaterials [4] have been developed in order to control the emissivity of a surface and consequently control the temperature of a body. Also, heavy devices such as thermal louvers [5] and morphable radiators [6,7] have been developed during the years in order to control the heat rejection in space applications. Both materials and systems present specific disadvantages in terms of weight, performance (thermal radiation leakages) and complexity. On the other hand, in Nature, thermal control of plants and other living organisms has been addressed through mechanistic design approaches. More specifically, thermonastic and photonastic movements are realized in order to transform the shape of leaves/petals under a temperature or light stimulus and to prevent overheating [8-10], because of the coexistence of two layers with different thermo-optical properties. The inner or outer layer of the plant is revealed or concealed in order to prevent over-heating/over-cooling [9,10]. Moreover, non-living tissues of various plants are designed to undergo predetermined shape transformations through the triggering of their fibrous, heterogeneous and multilayer structure [11], creating responsive materials that change their shape drastically. These responsive materials inspired numerus researchers to develop materials that change shape through the above-mentioned principles using hydrogels, polymers and other material in multilayer and anisotropic structure [12-15]

Combining the above-mentioned functions of plants (coexistence of coatings with different thermo-optical properties, and responsive materials), we designed ultralight smart surfaces that change their thermal radiation emissivity drastically for small temperature change. In the past, we developed smart surfaces that alter their effective emissivity drastically using multilayer and anisotropic responsive materials Fig. 1. Our preliminarily study showed that these smart surfaces present very low weight (the weight of the developed smart surfaces was less than 330 gr/m^2) and large emissivity change [15,16].

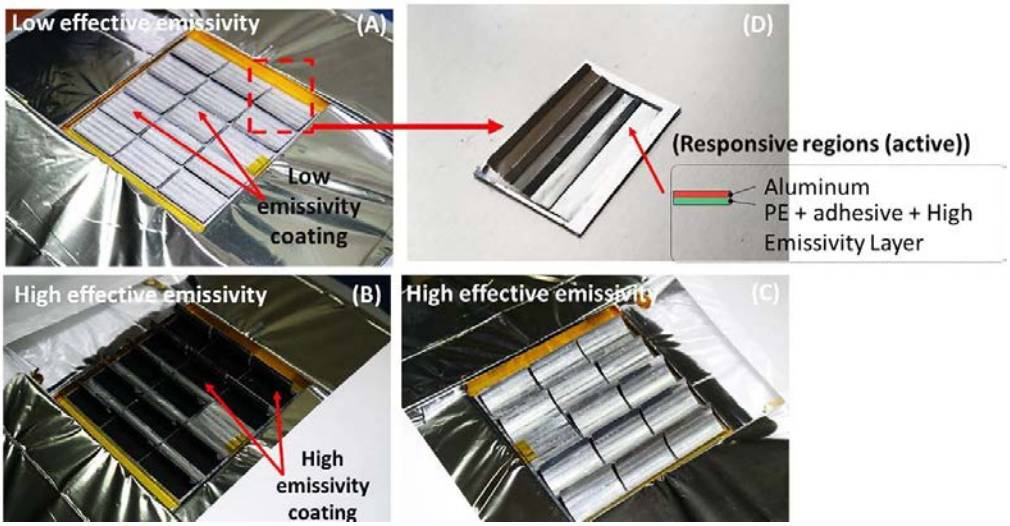

Figure 1: (A) Smart responsive surfaces (100mm x 100mm dimensions) at room temperature with low effective emissivity [16], (B,C) Smart surfaces at elevated temperature with high effective emissivity, (D) Unit-cell of the smart surface.

These smart surfaces consist of smaller unit-cells (Fig. 1D) and respond passively to temperature and thermal radiation. When the unit cells are in a closed position (Fig. 1A), the effective emissivity is low, because of the outer low-emissivity coating (silver colour). Increasing temperature level, all unit-cells open and reveal the internal high-emissivity coating Fig. 1B,C (black colour). Therefore, the effective thermal emissivity increases drastically. Their designed behaviour can be achieved through the prediction of their shape transformation by regulating the view factor of the patterned surface and the material (coating) that is exposed to the environment, creating smart materials with variable thermal radiation properties. The unit-cells transform their shape via the anisotropic material properties and the developed internal stresses, which occur because of the large mismatch in the coefficient of thermal expansion (CTE) of the multilayer material; the unit cells can perform very complex movements with large displacements and rotations. The high-CTE layer is a thermally-low conductive material (oriented HDPE "High density polyethylene"), whereas the low-CTE material is a thermally-high conductive material (Aluminium). Oriented HDPE presents extremely high CTE that varies with temperature, presenting also peculiar behaviour.

The scope of this study is four-fold: (A) the detailed FE modelling of the smart surfaces using thermally dependent material properties of the oriented HDPE in order to study the shape-change of the unit cells, (B) the prediction of the thermal emission behaviour and how the temperature dependent properties affect the performance, (C) the study of the temperature field of the responsive materials as a function of the thermal conductivity of the outer layer and its effect on the emission performance and power rejection, (D) the examination of the directional thermal emissivity versus temperature.

2 METHODOLOGY, GOVERNING EQUATIONS AND DETAILED MODELLING OF THE SMART SURFACES

The accurate prediction of the effective thermal emissivity of the smart surfaces is a difficult task due to the complex multiphysics phenomena, as well as the temperature dependent material properties. The proposed responsive smart surfaces consist of a highly oriented HDPE layer, a very thin layer of adhesive, an aluminium layer (low emissivity material), while the internal layer is a black mat coating (high emissivity). The oriented polyethylene presents very high CTE due to the molecular orientation, and the modulus of elasticity is strongly dependent on temperature. Therefore, the shape change sensitivity of the materials is strongly related with the temperature level, and their implementation is imperative.

2.1 Governing Equations of the thermo-mechanical problem

The smart surface of Fig. 1, was modelled as a plain-strain, geometrically non-linear problem. A heat flux (Q) was set below the smart surface. The steady-state temperature field of the smart surfaces was calculated as a function of the heat flux (Q); therefore, the effective emissivity could be calculated as a function of the temperature.

$$e_{el} = \frac{1}{2}\left[\left(\nabla u\right)^T + \nabla u + \left(\nabla u\right)^T \nabla u\right] - a_{(T)}\left(T - T_{ref}\right) \qquad (1)$$

A coupled thermo-mechanical and geometrically non-linear problem was solved, which would also incorporate the interactions of the body caused by thermal radiation.

Stresses are represented by the Second Piola–Kirchoff stress tensor; the strains are represented by the Green–Lagrange strain tensor, Eq. 1. The $CTE_{(T)}$ curve can be fitted/represented by Boltzmann fitting curve in order to implement temperature. The modulus of elasticity $E_{(T)}$ is also a function of temperature, and both parameters are dominant and affect significantly the final solution.

The CTE ($\boldsymbol{\alpha_{(T)}}$) of the oriented HDPE is expressed by a 2nd order tensor (α), Eq. 2, because of the anisotropic characteristics of the oriented HDPE.

$$\alpha_{(T)} = \begin{bmatrix} \alpha_{11(T)} & 0 \\ 0 & \alpha_{22(T)} \end{bmatrix} \qquad (2)$$

However, because of the plain-strain problem, it is necessary to implement only the $\alpha_{11(T)}$ parameter that lies on the principal axis. Because of the anisotropy and the local heterogeneities of the oriented HDPE, we decided to study the behaviour of the material using large specimens. An apparatus was manufactured and we measured the CTE using a laser setup, and we examined three samples as a function of temperature, Fig. 2A. An average Boltzmann fitting curve was used for the modelling, Fig. 2B.

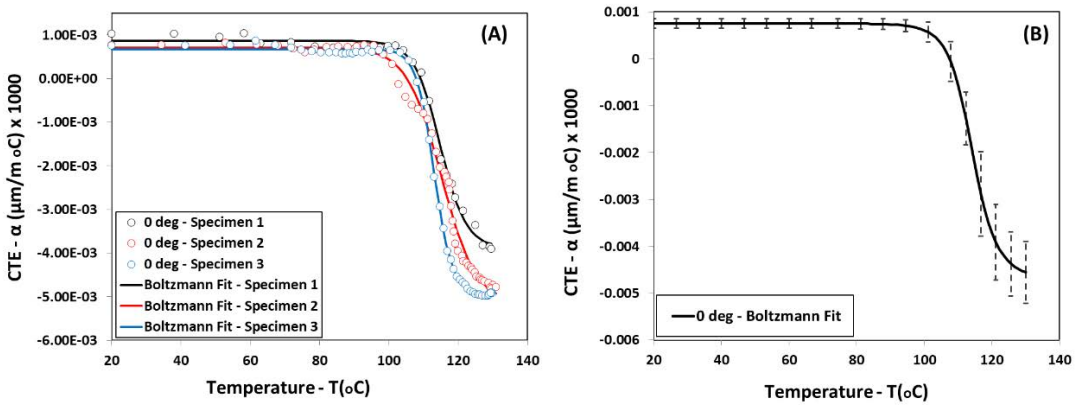

Figure 2: (A), CTE measurements of HDPE films using a high accuracy laser displacement and uniform temperature, (B) Averaging of measurements and fitting using Boltzmann formula, Eq. 3.

Boltzmann fitting formula is given by Eq. 3. All necessary parameters are presented in Table 1.

$$\alpha_{11(T)} = \frac{A_1 - A_2}{1 + e^{(T - x_o)/dx}} + A_2 \qquad (3)$$

Table 1. Fitting parameters of CTE $\alpha_{11(T)}$ according to Boltzmann formula (Eq. 3), and fitting parameters of the modulus (E) using an exponential function (Eq. 4).

A_1	7.46E-04	**B_1**	1.009 E9
A_2	-0.0046	**S**	52.819
x_o	114.062	**y_0**	-76.68 E6
dx	3.65526		
T	Temperature (°C)		

The modulus of elasticity of the HDPE film can be represented by an exponential fitting curve, Fig. 3. All fitting parameters have been included in Table 1.

$$E_{(\mathrm{T})} = B_1 e^{-(T/s)} y_0 \qquad (4)$$

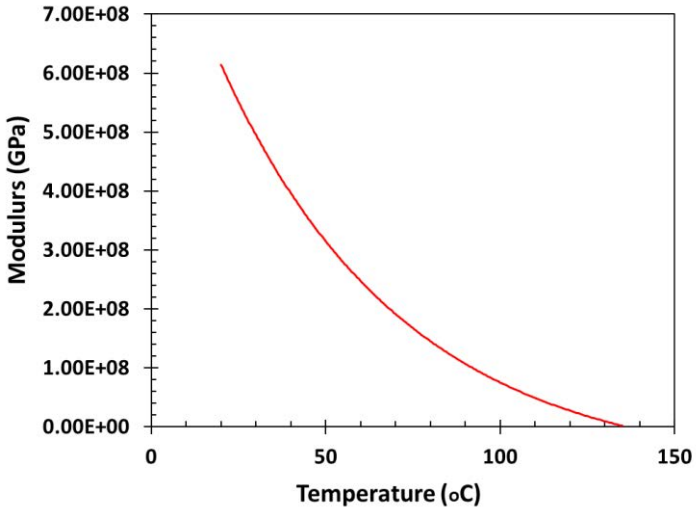

Figure 3: Modulus of elasticity of the HDPE film as a function of temperature [17].

Initially, the thermomechanical problem was modelled only for the unit-cell in order to study the shape-change of the multilayer material as a function of temperature. Figure 4 presents the real deformation versus the predictions using FEM for two different temperature levels. Structured quadrilateral elements were used for the modelling of the overall phenomenon, also taking into consideration the geometrical non-linearities. Hence, nonlinear terms and cross derivatives exist, which allow the large deformation of the elements to be expressed as a function of temperature. The thickness of the oriented HDPE film was 45μm and the thickness of the aluminum was 20μm.

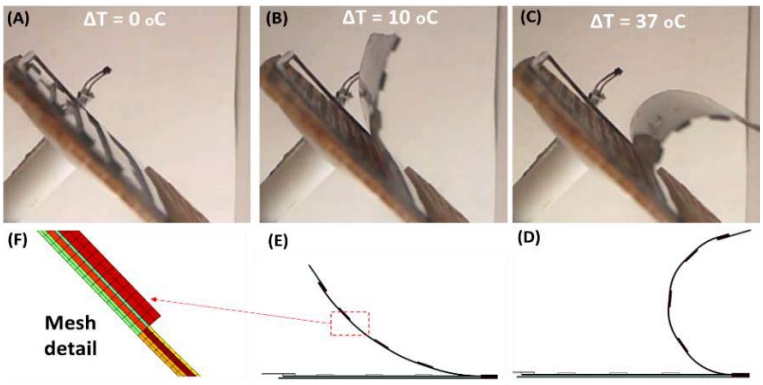

Figure 4: Unit cell deformation versus the FE predictions as a function of temperature.

2.2 Governing Equations of the thermal radiation problem

Assuming an ideal grey body, the radiosity leaving a surface is defined by Eq. (5) [16].

$$J_i = (1-\varepsilon_i)\left[G_{m,i}(J) + F_{a,i}\sigma T_\infty^4\right] + \varepsilon_i \sigma T_i^4, \qquad i = 1,\ 2,\ \ldots, N \qquad (5)$$

Where (ε_i) is the surface emissivity; (i) denotes the surface of the low- or the high-emissivity material. (F_a) is an ambient view factor, and (T_∞) is the assumed far-away temperature in the directions included in (F_a). (G_m) is the mutual irradiation from other boundaries. (N) expresses the number of surfaces of which the overall smart surface consists. As we have already mentioned, we modelled the plane strain problem of Fig. 5A. Therefore, we modelled five unit-cells in series and their interaction, Fig. 5B. On the internal surfaces of the unit cells, the emissivity is high ($\varepsilon_1 \approx 0.95$), and on the external surface of the unit cells, the emissivity is low ($\varepsilon_2 \approx 0.075$), Fig. 5A, B. The prediction of the transformed geometry of the smart surface and the temperature field for different heat fluxes allow us to calculate the effective emissivity using Eq. (6). For each steady-state position and temperature field, the effective emissivity can be calculated as follows:

$$\varepsilon_{eff} = Q / \sigma(T^4 - T_\infty^4) \qquad (6)$$

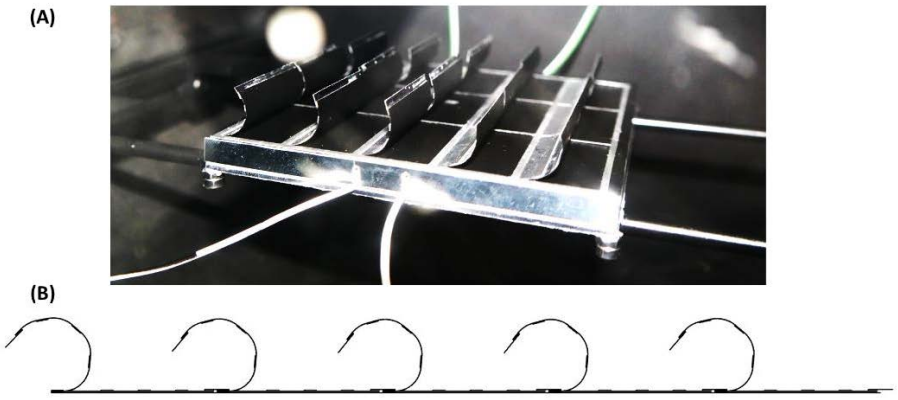

Figure 5: (A) Picture from the real experiment and the (B) deformed smart surface using coupled FEM.

3 RESULTS AND DISCUSSIONS

Through FE modelling, we calculated the effective emissivity as a function of temperature, for different programming temperature levels. Programming temperature means that the responsive material is flat in a specific temperature level. Above this temperature, the unit-cells are deformed similar to Fig. 5 and Fig. 6. E.g. we can set the programming temperature to be at 0 ^oC, at 40 ^oC or at -30 ^oC. Therefore, all unit-cells present flat geometry (closed position). If the programming temperature is high, the responsive unit-cells open differently because of the materials' property dependence, which alter also their performance.

Moreover, examining the temperature field of the responsive materials (arc, Fig. 5B), we studied how the thermal conductivity affects the overall performance of the heat rejection capability of the smart surface. Finally, we calculated the directional emissivity of the smart

surfaces in order to study the heat rejection direction as a function of temperature.

3.1 Prediction of the effective emissivity through coupled FEM

Figure 6A presents the calculated emissivity of the smart surfaces as a function of temperature. The minimum emissivity value was set at 13 °C. Below 13 °C, the emissivity remains constant. When temperature increases the unit cells open and the effective emissivity increases (red line). The red line presents the calculated effective emissivity versus temperature for a thermal conductivity of 205 W/mK. The emissivity changes its value by ($\Delta\varepsilon \approx 0.82$) within a temperature change of $\Delta T = 30.8$ °C, while the experimental results [16] dictate a change ($\Delta\varepsilon = 0.762$) within a temperature span of $\Delta T = 47.05$ °C (black dotted line). The comparison between the calculated and the measured effective emissivity is not excellent. However, the phenomenon and the model are very complex. Differences could be appeared because of the material properties change, manufacturing uncertainties and assumptions.

The important aspect is that the sensitivity the smart surface response changes because the CTE and modulus is strongly related with temperature, making the material more sensitive at lower temperature levels (dark red and dark purple lines, Fig. 6). The emissivity change is ($\Delta\varepsilon \approx 0.82$) within a temperature change of $\Delta T = 25.7$ °C (dark red line), while for initial temperature equal to 40ºC, the material is less sensitive and the emissivity change is ($\Delta\varepsilon \approx 0.805$) within a temperature change of $\Delta T = 41$ °C. In Figure 6B, we present the inclination of each curve in order to present the sensitivity as a function of temperature for different temperature levels. In any case, this difference should be taken into consideration in order to design a highly oriented film with a modulus of elasticity that is not affected by the temperature level drastically.

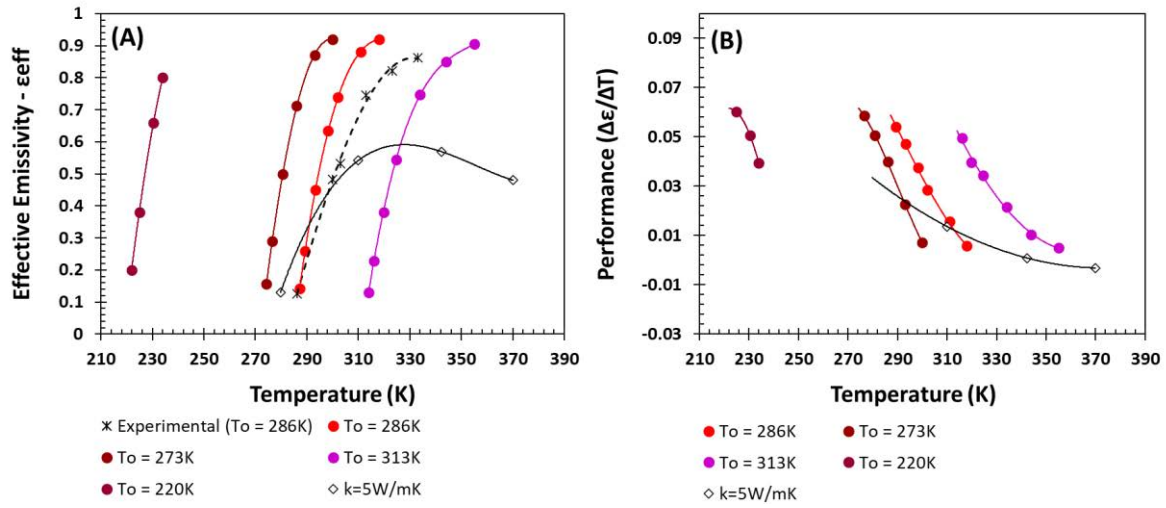

Figure 6: (A) Calculated effective emissivity as a function of temperature for different programming temperature levels. The experimental curve is presented as a comparison [16]. (B) Performance and sensitivity of smart surfaces for different programming temperature levels.

3.2 Temperature field as a function of the thermal conductivity

The heat rejection performance of the smart surfaces is strongly related with the scale of the unit cells. Because of the macro-scale design, the heat should be transferred and rejected by the responsive layers. We should stress that the presence of the aluminium or any other highly conductive material is imperative, because the material presents a uniform temperature field and deformed symmetrically without significant shading of the neighbour unit cells, Fig. 7A.

Calculating the effective emissivity as a function of temperature using materials with low thermal conductivity (5 W/mK). The emissivity changes only by ($\Delta\varepsilon$ = 0.45) within a temperature span of ΔT = 49 ºC (black line, Fig. 6A).

When the outer surface consists of materials with low thermal conductivity, the heat rejection is prevented because the energy cannot be transferred and the tip of the unit cells presents lower temperature levels, while the base of the unit cell presents much higher temperature level. As a consequence, the unit-cells deformed as shown in Fig. 7B, and shades the neighbour unit cell.

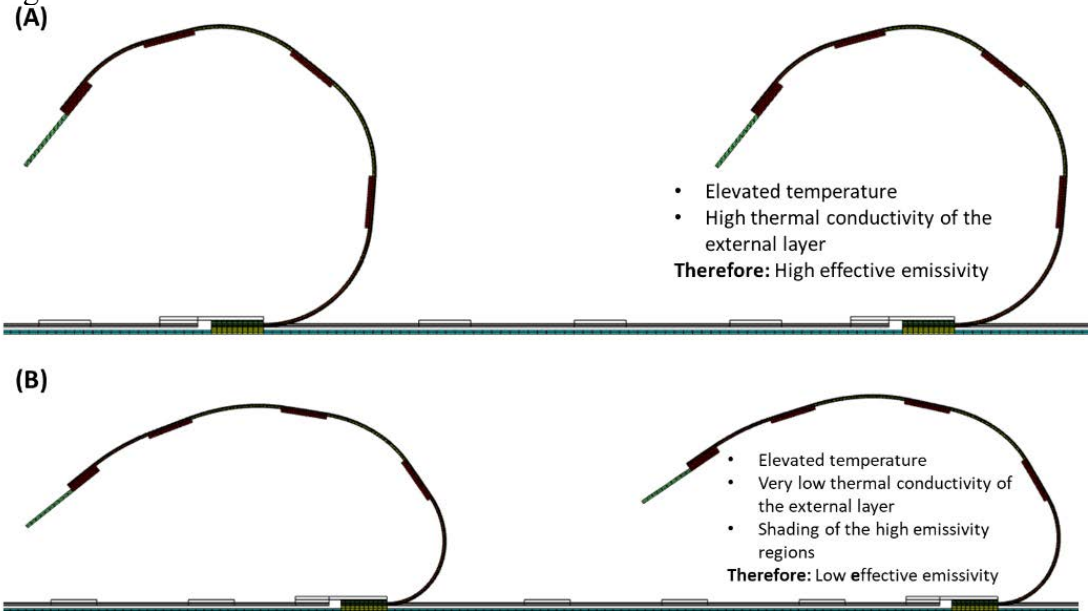

Figure 7: (A) Deformation of the unit-cells with high thermally conductive outer layer, (B) Deformation of the unit-cells with very low thermally conductive outer layer. We present only two, out of the five unit-cells.

The rejection of the thermal energy is reduced drastically as the thermal conductivity is decreased. The low thermal conductivity does not allow the conductive heat flux to reach the edge of the unit cell, FIG. 8A. Large temperature deviation (19 ºC) are observed along the length of the unit cell (solid lines) for any power level. The capability of the surface to reject thermal energy has been mitigated owing to the low temperature values at the edge of the deformable unit cells. In contrast, high thermal conductivity values lead to a uniform temperature field along the length of the unit-cell with temperature deviation less than (1.5 ºC), and the rejection of the thermal energy is maximised.

A In Fig. 8B, we present the calculated effective emissivity as a function of power for

different thermal conductivity values. The red line shows that for high power levels (>250W/m^2) the emissivity is reduced due to the extremely deformed geometry.

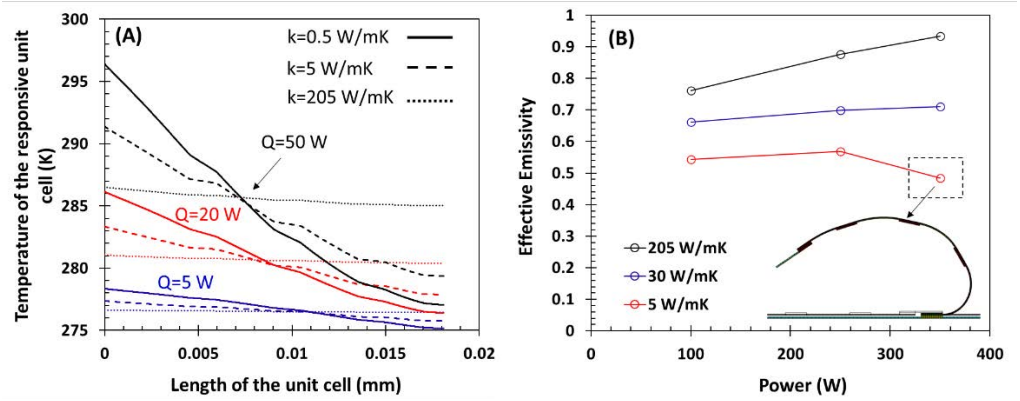

Figure 8: (A) Temperature field of the responsive region of the unit cell as a function of the thermal conductivity of the outer layer and the power. (B) Effective emissivity as a function of the power and the thermal conductivity.

3.3 Directional emissivity of the smart surfaces as a function of temperature

Our aim is to study the angular distribution of the intensity of folded arrays as a function of temperature (T). The angular distribution of the intensity for all the wavelengths was calculated for the azimuthal and polar direction for different Ω angles. The Ω angle denote the angle of the folded arrays and is a function of temperature $\Omega_{(T)}$. Each structure emit energy to all directions and wavelengths as a function of temperature according to the geometrical characteristics and the materials that have been applied on the external and internal surfaces, total hemispherical emissivity $\varepsilon_{(T)}$. Each structure emits thermal energy as a function of the azimuthial angle (Θ), polar angle (Φ) and the folding angle ($\Omega_{(T)}$), Fig. 9A. Therefore, the directional radiative heat flux is a function of three different parameters (Θ, Φ, $\Omega_{(T)}$).

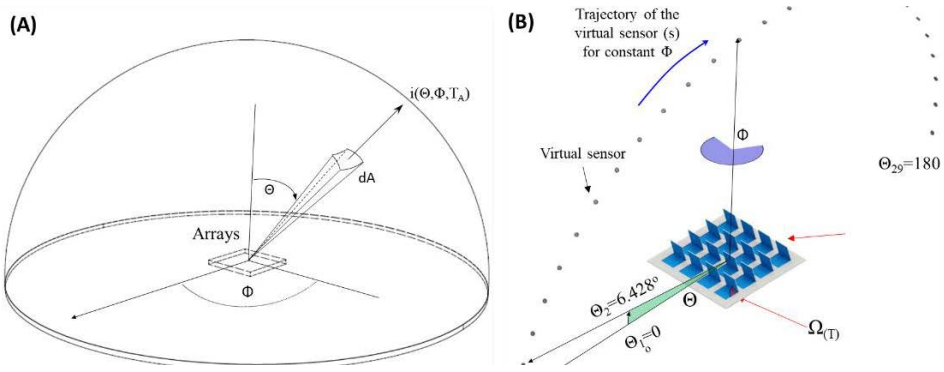

Figure 9: (A) Θ represents the polar angle and Φ represents the azimuthal angle; (B) Spatial position of the artificial sensor as a function of (Θ, Φ) for the calculation of the directional emissivity $\varepsilon_{(\Theta,\Phi)}$ as a function of the angle $\Omega_{(T)}$ of the smart structure. (Ω) represent the angle of the smart structure for any temperature level (T). The sensor scans the hemisphere from angle $\Theta_1 = 0^o$ to angle $\Theta_{29} = 180^o$ with an interval of $\Delta\Theta = 6.428^o$ as well as from angle $\Phi_1 = 0^o$ to angle $\Phi = 180^o$ with an interval of $\Delta\Phi = 15^o$.

A virtual sensor scans the entire hemispherical surface in intervals $\Delta\Theta = 6.428^{o}$ and $\Delta\Phi = 15^{o}$ (Fig. 9B). Calculating the temperature of the virtual sensor through the 3D numerical models, we can extract the angular intensity for any pair of (Θ, Φ). The directional thermal emission (Q) was determined for all the combination of azimuthial, polar angle and temperature levels (Ω angles), Eq 6. In order to construct the polar diagrams, 135 problems were solved for each Ω angle.

$$a_{vs}Q_{(\Theta,\Phi,\Omega)} = \varepsilon_{vs}\sigma(T^4 - T_{\infty}^4) \qquad (7)$$

The absorptivity (α_{vs}) and the emissivity (ε_{vs}) values of the virtual sensor are equal to one. On the internal regions of the unit cells, the emissivity is high ($\varepsilon_1 \approx 0.95$), and on the external surface of the unit cells the emissivity is low ($\varepsilon_2 \approx 0.075$). Moreover, the directional emissivity of the aluminum is assumed to be constant.

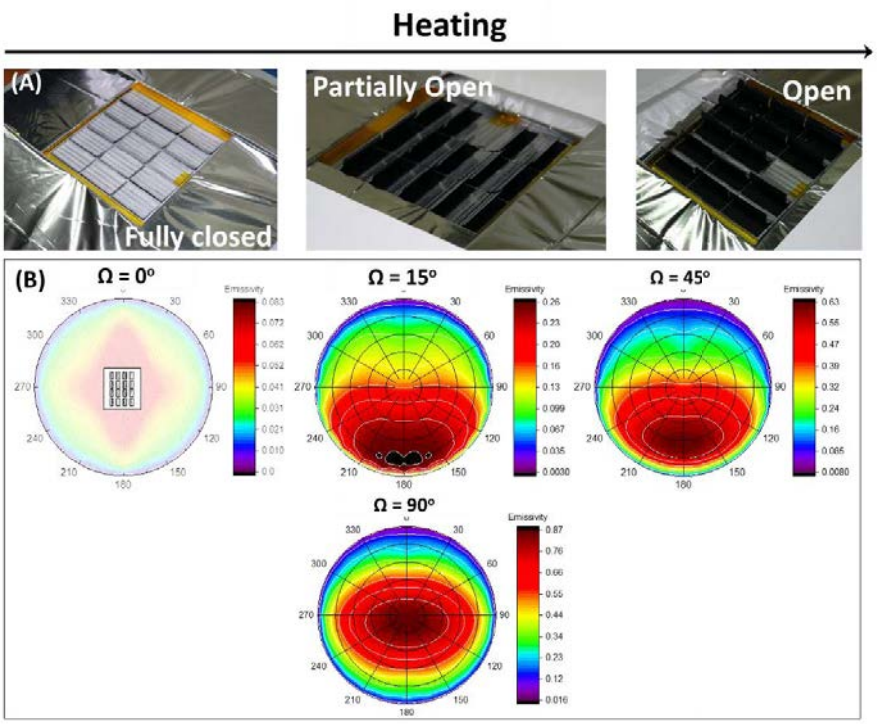

Figure 10: (A) Smart surface response at elevated temperature. (B) Directional emissivity maps for $\Omega = 0^{o}$, $\Omega = 15^{o}$, $\Omega = 45^{o}$, $\Omega = 90^{o}$.

Figure 10B presents the intensity of the smart surface during the transformation of the arrays' geometry, FIG. 10A. The total hemispherical emissivity at $\Omega = 0^{o}$ is very small and equal to the emissivity of the external aluminum coating (ideal scenario). As the temperature increases the unit cells of the smart surface open. During the transformation, the total hemispherical emissivity increases because the area of revealed internal coating dominates. Moreover, the maximum intensity value changes direction (Θ and Φ). Each Ω Angle generates unique angular distribution intensity maps. In FIG. 10B ($\Omega = 0^{o}$), the directional emission is uniform, while at

$\Omega = 15^o$ the thermal emission is directed only to a minor region. Similar behaviour is observed for $\Omega = 45^o$ while the effective emissivity increases because of the larger deformation of the unit-cells. At $\Omega = 90^o$ the emissivity value lies near the maximum effective emissivity value.

This analysis dictates that the smart surfaces interact with the environment directionally. Hence, the surface could emit in a specific direction and reflect the heat from another direction. Consequently, each structure presents unique characteristics regarding the directional dependency with an outer heat source. Also, the proposed smart surfaces could be used for the identification of the heat source direction. The scope of this analysis is not related with the extensive study of the structures as sensors, but to reveal parameters that govern the behaviour of the smart surfaces.

4 CONCLUSIONS

The proposed smart surfaces are capable of performing complex movements with large deformations. Using common/commercial multilayer anisotropic materials, we can develop responsive smart surfaces that control the temperature of a body. Oriented HDPE is a very good candidate because presents very high CTE values, from ≈650 x 10^{-6} m/m ^oC to ≈1000 x 10^{-6} m/m ^oC. Through the study and implementation of temperature dependent material properties (CTE and Modulus), we predicted the shape and the effective emissivity as a function of temperature. We studied the sensitivity for different temperature levels, and we concluded that for lower temperature levels the material is more effective. In any case, the material reacts efficiently over a very broad range of thermal requirements. However, higher sensitivity for higher temperature levels would be essential. For this reason, the design of a highly oriented film with a modulus of elasticity and CTE that are not affected drastically by the temperature level, is imperative.

The thermal conductivity of the outer layer affects significantly the shape of the unit cells and the overall performance of the smart surface. Polymeric materials with metallic thin coatings could function properly as outer surfaces. For this reason, metallic foils or thick coatings are advantageous.

Finally, we should stress that these smart surfaces emit the thermal energy in specific directions according to the deformation of the unit cells. This characteristic could be used in order to emit in a specific direction and reflect the heat from another direction.

Probably, space applications could be an appropriate sector in order to implement these materials and technology.

ACKNOWLEDGEMENTS

This research is funded and implemented through the *"3rd Call for H.F.R.I. Research Projects to Support Post-Doctoral Researchers"* in Greece, under the name INTEGRAL with project ID: 7401 and Reference Number 49597 - 24/05/2022.

CONTRIBUTIONS

The manuscript was written mainly by N. A. The central methodology and the experiments were conducted by N. A. N.A. and G. C. formulated the thermomechanical FE models. N. A. formulated the coupled thermomechanical and thermal radiation FE models. N. A. and N.J.S.

formulated the steady-state FE models for the investigation of the directional thermal emissivity.

5 REFERENCES

[1] M. A. Kats, et al. Vanadium dioxide as a natural disordered metamaterial: Perfect thermal emission and large broadband negative differential thermal emittance, *Physics Review X*, Vol. 3, pp. 1–7, 2014.

[2] S. Tachikawa et al., Development of a Variable Emittance Radiator Based on a Perovskite Manganese Oxide. *Journal of Thermophysics Heat Transfer,* Vol. 17, pp. 264-268, 2003.

[3] S. Cao, et al. Variable emissivity surfaces for micro and Nano-satellites, *Physics Procedia*, Vol. 18, pp. 91–94, 2011.

[4] T. Inoue, M. De Zoysa, T. Asano and S. Noda, Realization of dynamic thermal emission control. *Nature Materials,* Vol. 13, pp. 928–931, 2014.

[5] D. G. Gilmore, *Spacecraft Thermal Control Handbook Volume I: Fundamental Technologies*, The Aerospace Press, 2002.

[6] H. Nagano, A. Ohnishi and Y. Nagasaka, Development of a lightweight deployable/stowable radiator for interplanetary exploration. Appl. Therm. Eng. 31, 3322–3331, 2011.

[7] Cognata, T. J. et al. A Morphing Radiator for High-Turndown Thermal Control of Crewed Space Exploration Vehicles, *23rd AIAA/AHS Adaptive Structures Conference*, 1509, 2015.

[8] P. Tao et al, Bioinspired engineering of thermal materials, *Advanced Materials,* Vol. 27, pp. 428–463, 2015.

[9] E. T. Nilsen, Why Do Rhododendron Leaves Curl, *Journal American Rhododendron Society,* Vol. 40, pp. 31–35, 1986.

[10] C. Ye, et al, Highly reflective superhydrophobic white coating inspired by poplar leaf hairs toward an effective 'cool roof'. *Energy & Environmental Science,* 4, 3364, 2011.

[11] C. Dawson, J. F. V. Vincent and A.-M Rocca, How pine cones open, *Nature*, 390, 668, 1997.

[12] R. M. Erb, J. S. Sander, R. Grisch, A. R. Studart, Self-shaping composites with programmable bioinspired microstructures*, Nature Communications*, Vol. 4, 1712, 2013.

[13] S. Gladman, A., Matsumoto, E. A., Nuzzo, R. G., Mahadevan, L. & Lewis, J. A. Biomimetic 4D printing. Nat. Mater. 15, 413–8 (2016).

[14] Q. Zhao, W. Zou, Y. Luo and T. Xie, Shape memory polymer network with thermally distinct elasticity and plasticity, *Science Advances,* Vol. 2(1), e1501297, 2016.

[15] N. Athanasopoulos and N. J. Siakavellas, Smart patterned surfaces with programmable thermal emissivity and their design through combinatorial strategies, *Scientific Reports*, 7, 12908, 2017.

[16] N. Athanasopoulos and N. J. Siakavellas, Variable emissivity through multilayer patterned surfaces for passive thermal control: preliminary thermal design of a nano-satellite, 48th International Conference on Environmental Systems, ICES-2018-296, 8-12 July 2018, Albuquerque, New Mexico.

[17] N. Merah et. al, Temperature and loading frequency effects on fatigue crack growth in HDPE pipe material, Arabian Journal for Science and Engineering ,31(2):19-30, 2006.